**TESLA-FEL 2008-06**

# Efficacy testing of shielding materials for XFEL using the radiation fields produced at FLASH

**Bhaskar Mukherjee, Evgeny Negodin, Thomas Hott and Stefan Simrock**

Deutsches Elektronen-Synchrotron (DESY), Notkestraße 85, D-22607 Hamburg, Germany

**Email**: mukherjee@ieee.org

## EXECUTIVE SUMMARY

The European X-Ray Free Electron Laser (XFEL), a grand international scientific endeavour to produce extremely brilliant (~ $10^{33}$ photons/s/mm$^2$/mrad$^2$), ultra short pulsed (~ 100 fs) coherent X-rays of wavelengths down to 0.1 nm is now under construction at DESY (Deutsches Elektronen-Synchrotron) laboratory. The XFEL facility, which measures a total length of 3.3 km will be driven by a 1.7 km long, 20 GeV electron linac made of high-purity superconducting niobium cavities developed at DESY under TESLA (Tera Electron-Volt Superconducting Linear Accelerator) technology collaboration. The electron linac section of the XFEL will be housed in a 5 m diameter underground concrete tunnel. Furthermore, all electronic equipments vital to machine safety, operation and control system of the linac, as well as the klystrons and power supplies will also be installed in the tunnel. Intense field of parasitic (ionising) radiations will be generated during linac operation thereby causing radiation induced detrimental effects in the electronic devices. Hence, in order to guarantee a safe and flawless linac operation, it is imperative to implement suitable radiation shielding around the racks containing those electronic equipments.

Radiation shielding design for the electronics operating in close vicinity of a high-energy electron linac, installed in a narrow 5 m diameter tunnel is complex and has to cope with the following major challenges: (**a**) Due to space limitation in the tunnel, a compact shielding is mandatory, i.e. provision of a maximum radiation attenuation at the location of interest with a minimum shield thickness and (**b**) extremely complex radiation exposure geometry and large variation of linac operation conditions make the shielding calculations based on Monte-Carlo simulation unsuitable to produce reliable results. We have therefore, adopted the analytical calculation method using the results of radiation measurement experiments at Free Electron Laser in Hamburg (FLASH), already operational at DESY. The optimum photon shielding parameters for selected materials were calculated.

This report highlights experimental methods to estimate the photon (bremsstrahlung gamma rays) and neutron field distributions along FLASH tunnel. Photon attenuation (shielding) parameters in industrial lead, carbon steel, heavy concrete and multi-layer shield (lead + heavy concrete) are presented. Application of this evaluated data for the construction of optimised shielding of electronics racks to be installed in XFEL tunnel is recommended.

# INTRODUCTION

XFEL facility is broadly configured in three parts. (**a**) The injector building, to be located at the north-west site of the DESY laboratory. (**b**) Accelerator (20 GeV electron linac) tunnel, a 1.7 km long, 5 m diameter concrete tunnel placed at least 6m underground. (**c**) The accelerator tunnel will be followed by two undulator tunnels leading to experiment halls. The XFEL facility construction plan is documented in details elsewhere [**1**].

The main objective of our investigations deals with experimental estimation of attenuation properties of selected materials to be used in the construction of optimised radiation shielding for the electronic equipment racks installed in the XFEL-linac tunnel (**Figure 1**).

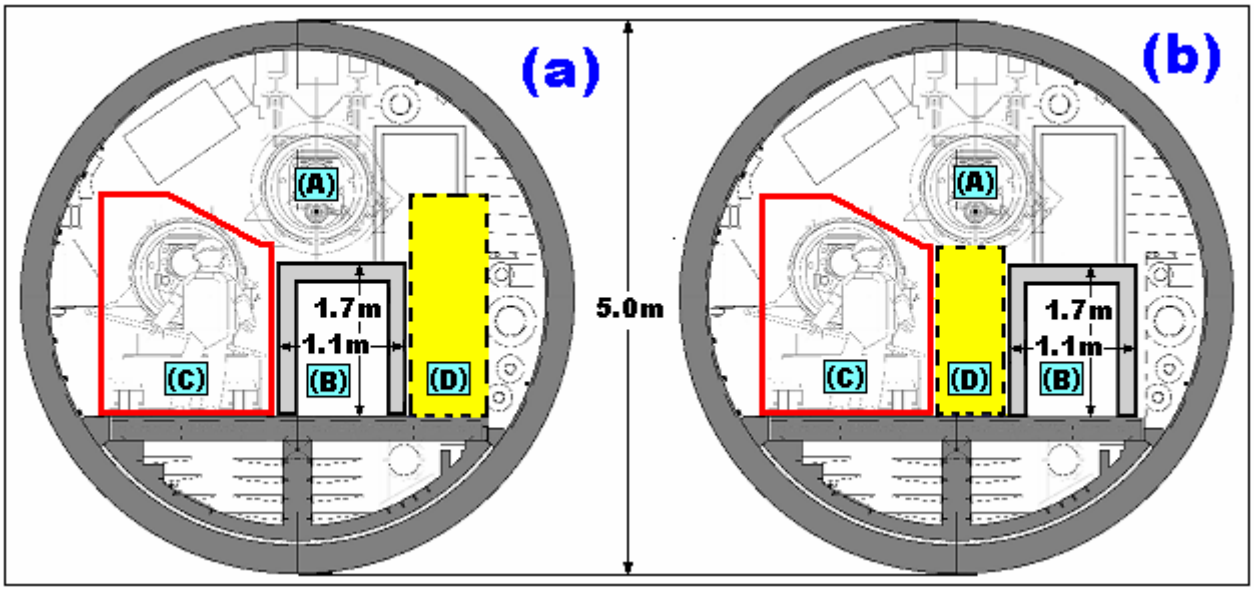


**Figure 1:** Cross sections of XFEL-linac tunnel highlighting the position of the accelerator module (**A**), shielded space of a cross section 1.7 × 1.1 $m^2$ allocated for electronics racks and other ancillaries (**B**), space allocated for passage of maintenance and fire safety equipments (**C**), and personnel movement and emergency escape passage (**D**).

The cross section of the linac tunnel in Figure 1(a) showing the location of shielded space (B) directly under the accelerator module (A). This configuration intended for the installation of klystrons and RF power supplies [**2**]. The tunnel cross section in Figure 1(b) indicates a shielded area close to the tunnel wall, will be used to house the racks for various electronic equipments, in particular the LLRF and linac control systems [**3**].

It is evident that the linac tunnel will be highly jam-packed with many equipments, utility ducts for water, compressed air, liquid helium, optical and signal cables, different electronic components and racks of various shapes, made of different materials (**Figure 1a, 1b**). Hence, an accurate Monte-Carlo simulation of the radiation transport (shielding attenuation), taking into account all the above objects (geometry) will be too complex, requiring a very long computing time. We have therefore, adopted an analytical method based on the data collected from radiation measurement experiment at FLASH. The parasitic radiations from a superconducting linac are primarily generated by accelerated field emission electrons and dark current, and depend on voltage gradient across the accelerating cavities [**4**]. As both FLASH and XFEL are made of same type of superconducting TESLA cavities, one can parameterise the radiation source terms from FLASH and apply them in the shielding calculations relevant to XFEL [**5**]. This vindicates our shielding assessment methods for electronic equipment for XFEL as highlighted in this report.

# MATERIALS AND METHODS

## Photon Dose Distribution along the Linac

The photon (gamma) dose distribution along the linac driving FLASH was estimated using radiochromic film dosimeters developed at our laboratory [**4, 6**]. Schematic diagram of FLASH facility, dosimetry locations and space for shielding materials test are depicted in **Figure 2**.

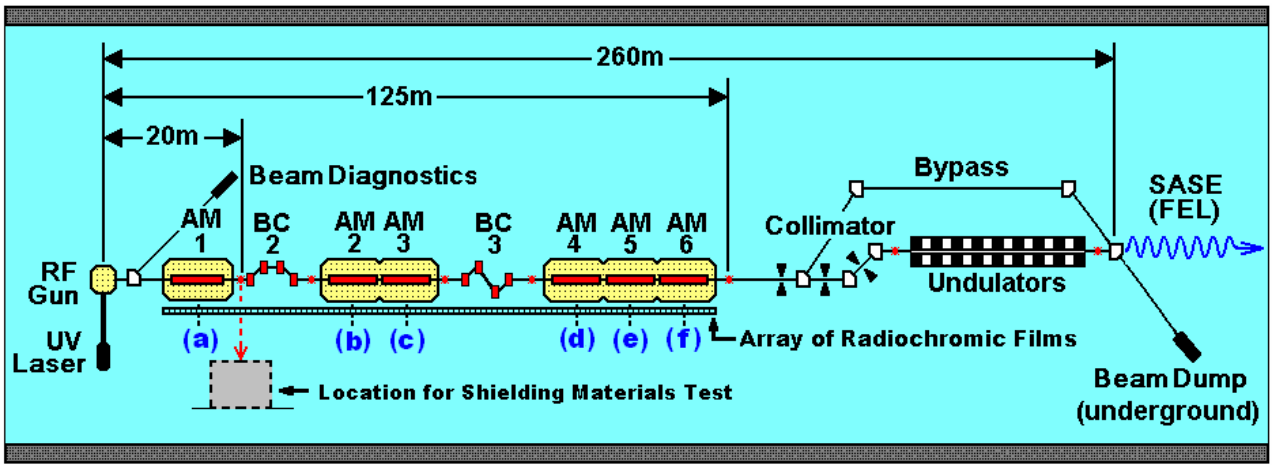


**Figure 2:** Schematic diagram of FLASH facility highlighting the gamma and neutron dosimetry spots and the location allocated for shielding material test.

Radiochromic (Type: GaF-EBT, Manufacturer: ISP, New Jersey, USA) film dosimeters were attached on the outer surface of the accelerator modules AM1 - AM6 and bunch compressors BC2 - BC3 and exposed during a routine FLASH operation period of three weeks. The films were evaluated [**4**] thereafter to estimate the gamma dose rates. The results are depicted in **Figure 3**.

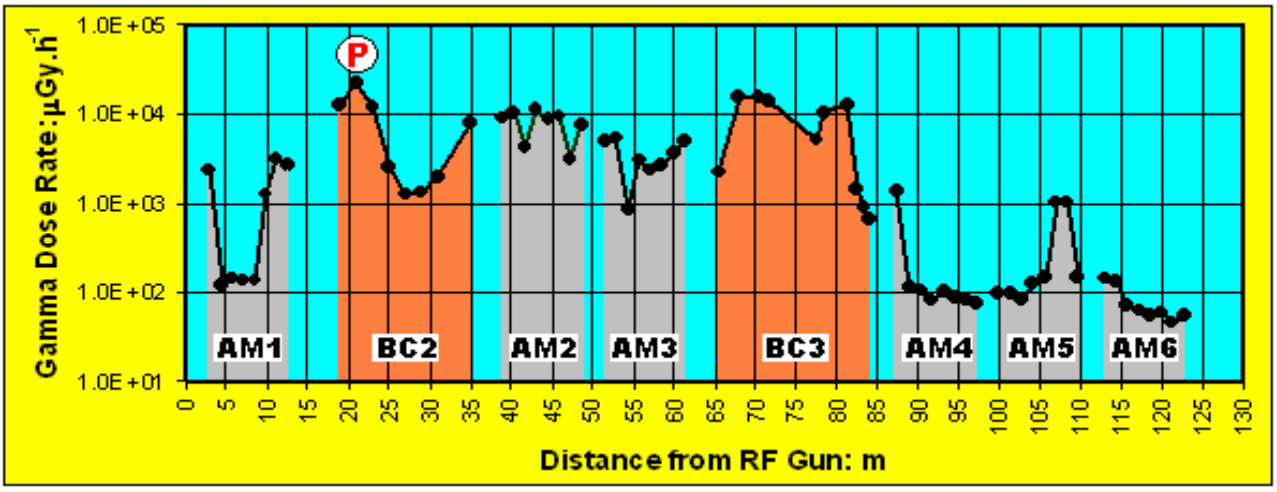


**Figure 3:** Gamma dose rate along the superconducting linac driving FLASH evaluated with radiochromic films and plotted against the distance from the reference point (RF Gun). The region of highest gamma dose rate is indicated (P).

## Neutron Kerma and Photon Dose Distribution near Accelerator Modules

Previous radiation measurement studies have revealed that a significant photoneutron production takes place near the accelerator modules operating a gradient higher than 16MV.m$^{-1}$[**4, 7**]. We have used the Neutron-Gamma Area Monitor [**8**] made of two pairs of TLD-600 and TLD-700 thermoluminescent dosimeter chips enclosed in a cylindrical polyethylene moderator (20 cm × 20 cm diameter) to estimate the neutron kerma and gamma dose rates.

A batch of six moderator cylinders (a), (b), (c), (d), (e) and (f) were placed close to centre of each accelerator module (**Figure 2**). The cylinders were exposed simultaneously with the radiochromic films during three weeks routine FLASH operation. The TLD chips evaluated according to the procedure described elsewhere [**8**]. The gamma dose rates and neutron fluence rates were estimated from TLD-700 and TLD-600 readings respectively. The neutron kerma rates in Silicon (building material of electronic components) were computed using the fluence to kerma conversion factor in Silicon [**9**]. Results are depicted in **Figure 4**.

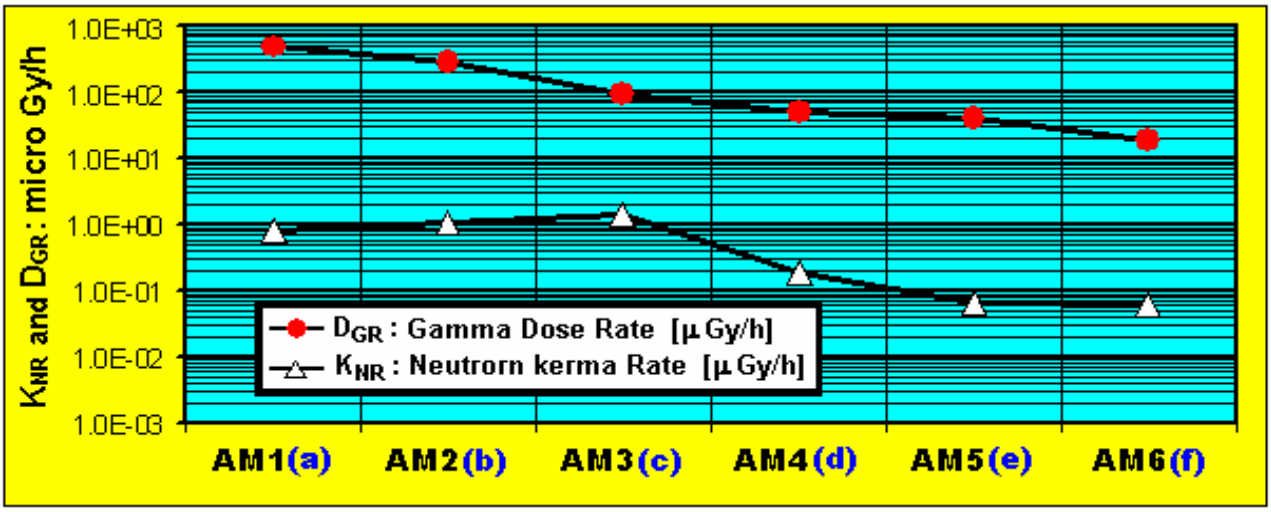


**Figure 4:** Gamma dose rate ($D_{GR}$) and neutron kerma rate ($K_{NR}$) near the superconducting accelerator modules AM 1 - AM 6 evaluated using TLD-600 and TLD-700 thermoluminescent dosimeter pairs enclosed in polyethylene moderator cylinders.

## Spatial Distribution of Radiation Field

Radiation measurement along FLASH tunnel revealed the highest gamma dose in the region between AM1 and BC2 (**Figure 3**). Hence, we have selected that location (**Figure 2**) for the testing of various shielding materials as described in this report. The spatial distribution pattern of gamma rays in the shielding measurement space was experimentally estimated (**Figure 5**).

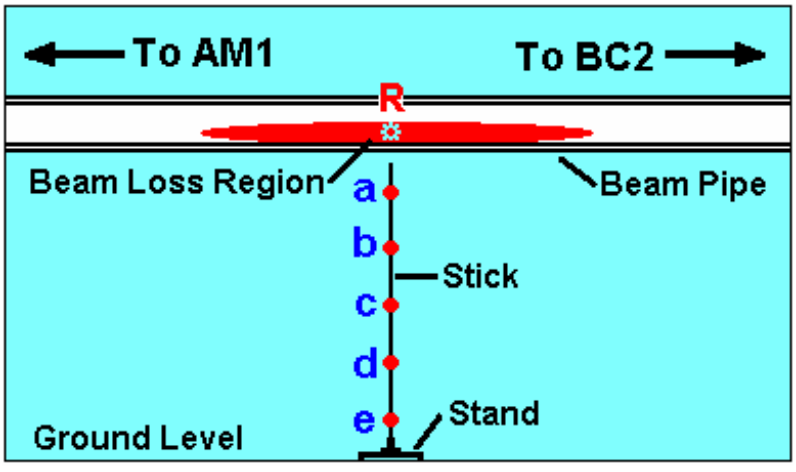


**Figure 5:** Schematic diagram of the experimental set up for the estimation of spatial distribution of the gamma radiation field at the location of shielding measurements, situated between the accelerator module AM1 and bunch compressor BC2.

Five pieces of radiochromic film dosimeters (a, b, c, d, d, e) were attached to a stick, at a distance of 10 cm between each film. The stick was installed on a stand near the beam-loss region (Figure 5) at the beam pipe section, connecting accelerator module (AM1) and bunch compressor (BC2).

A reference dosimeter [R] was placed directly on beam pipe at the Beam Loss Region. After two weeks routine operation of FLASH, the dosimeters were removed and evaluated using the procedures described elsewhere [**4, 6**]. The results are displayed in **Figure 6**.

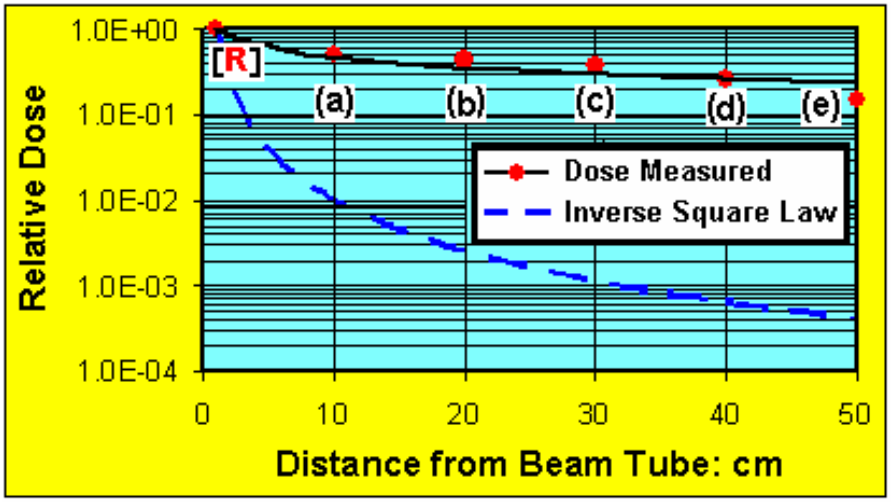


**Figure 6:** Photon dose distribution in free air, laterally along the beam pipe at locations (a), (b), (c), (d) and (e) (Figure 5) evaluated using radiochromic film dosimeters. The dose distribution calculated according to inverse square law is also indicated.

## Unfolding of Photon Energy Spectrum

The photon energy distribution (bremsstrahlung spectrum) at the location of shielding measurement (Figure 2) was experimentally estimated. Pieces of radiochromic films were placed under a stepped wedge (Material: Lead, $\rho = 11.3$ g.cm$^{-3}$) of thicknesses 0.5 mm, 1.0 mm, 2.0 mm, 7.0 mm, 12.0 mm, 17.0 mm and 22.0 mm. The system was exposed to gamma rays during three week routine operation of FLASH. The radiochromic films were evaluated [**4**, **6**]. From the optical densities of the films the transmitted gamma dose through all seven steps of the Pb-wedge was calculated. To unfold the bremsstrahlung spectrum a novel inverse calculation method, utilising the transmitted gamma doses through the stepped Pb-wedge, based on a Genetic Algorithm was used [**10, 11**]. The unfolded bremsstrahlung spectrum is shown in **Figure 7**.

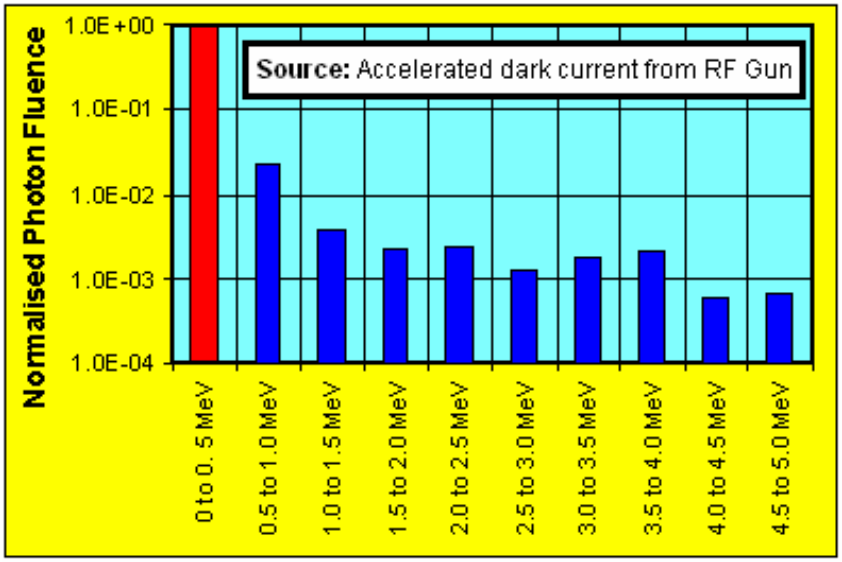


**Figure 7:** Unfolded bremsstrahlung spectrum evaluated from gamma (photon) doses transmitted through the stepped-wedge (0.5 mm, 1.0 mm, 2.0 mm, 7.0 mm, 12.0 mm, 17.0 mm and 22.0 mm) made of lead.

# INTERPRETATION OF EXPERIMENTAL RESULTS

The radiation measurement data collected from the above mentioned experiments at FLASH constitute the basis of the efficacy testing of selected shielding materials and optimised shielding design for the electronic equipment racks to be installed in the XFEL tunnel.

The gamma dose rates measured along the linac driving FLASH show the highest values near the region close to the bunch compressors and drop consistently with the distance from the reference point, i.e. the RF Gun (Figure 3). This invariably confirms the accelerated dark current (electrons) from the RF gun to be the major cause of the gamma radiation. The gamma dose rates at the modules AM5 and AM6, far away from the RF Gun, measured to be more than two orders of magnitude lower than the peak (P) dose measured at the bunch compressor BC2. High gamma doses were measured near the cavities 6 and 7 of accelerator module 5 (AM5). Evidently, this discrepancy was caused by the high field emission (electron) from those cavities. This high dose incidence could be eliminated/minimised either by switching off (detuning), or by reducing the gradient across those cavities [**4, 5**]. The gamma dose rates measured along the FLASH linac tunnel could be applicable to XFEL with appropriate parameterisations [**12**].

Neutron kerma and gamma dose rates at all six accelerator modules (AM1-AM6) evaluated using TLD-600 and TLD-700 thermoluminescent dosimeter pairs enclosed in polyethylene moderator cylinder reveal that neutron kerma rates measured to be more than two orders of magnitude lower than gamma dose rates (**Figure 4**). It is worth mentioning that in our case, both neutron kerma and gamma dose rates were calculated for Silicon (Si), the primary building material of all micro and macro electronic components. These results validate that the radiation environment of FLASH as well as XFEL is dominated only by photons. Consequently, the detrimental radiation damage in electronics is caused by the Total Ionising Dose (TID) effect of photons. Radiation damage due to Non Ionising Energy Loss (NIEL) effect from neutrons (also known as Displacement Damage) will be negligible, hence, could be ignored. Therefore, the main objective of this shielding research focused on photon (gamma) shielding.

The spatial distribution of gamma radiation field (relative dose) along the lateral direction from the radiation source, i.e. beam loss region R (**Figure 5**) show very little change with increasing distance. For example, at a distance of 30 cm the measured dose drops to a factor 0.3, whereas, the dose reduction according to inverse square law (assuming a point size radiation source) was calculated to be 0.001 (**Figure 6**). Hence, one can evidently conclude that the shape of gamma radiation source is not concentrated in a small region (point source) but widely distributed throughout the beam loss region.

The bremsstrahlung (gamma rays) spectrum at the location of shielding materials under test (**Figure 2**) was analysed from the evaluated photon dose, transmitted through an array of lead plates (stepped wedge) of different thicknesses. The inverse calculation method based on a Genetic Algorithm was used for the unfolding. The spectrum, within the energy range of 0.5 MeV - 5.0 MeV was divided into ten photon energy bins of 0.5 MeV width. The unfolded bremsstrahlung (gamma) spectrum (**Figure 7**) confirms that more than 90% of the spectrum is confined within the energy bins 0.5 -1.0 MeV. The peak and average bremsstrahlung photon energy calculated to be 0.5 MeV and 0.9 MeV respectively. The bremsstrahlung spectrum (photon energy distribution) could be used for analytical calculation of shielding parameters of material of interest.

# SHIELDING EFFICACY MEASUREMENT

## Principle of Shielding Calculation

We have adopted the analytical shielding calculation method originally developed for photon shielding analysis at SLAC [**13**]. The principle of shielding calculation is described in **Figure 8**.

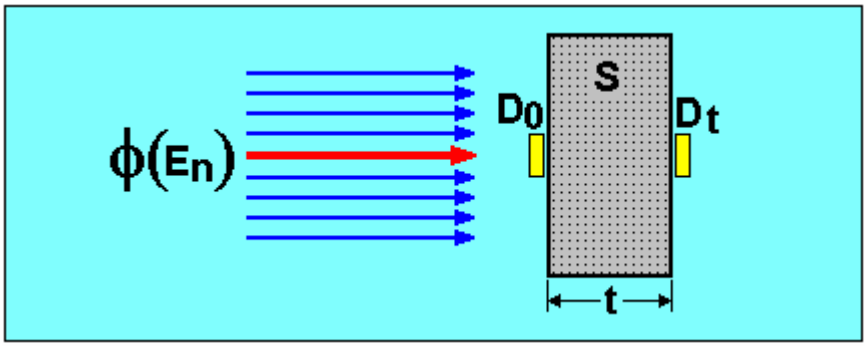


**Figure 8:** Showing the principle of shielding calculation using analytical method.

The incoming beam of photons with the spectral distribution $\phi(E_n)$ impinges on the shielding (S) of thickness (t). The gamma doses at the entrance (pre shielding) and egress (post shielding) sides are given as $D_0$ and $D_t$ respectively. The photon transmission factor ($D_t/D_0$) of the shielding of interest is given as:

$$\left(\frac{D_t}{D_0}\right)_{NBU} = \sum_{i=1}^{i=n} e^{-\mu_i t} \qquad (1)$$

$$\left(\frac{D_t}{D_0}\right)_{BU} = \sum_{i=1}^{i=n} B_i e^{-\mu_i t} \qquad (2)$$

Equation (1) represents the photon transmission through the shielding for a narrow photon beam (marked in red in Figure 8) without dose build up (**NBU**). On the other hand Equation (2) represents photon transmission for a broad photon beam (marked in blue in Figure 8) with dose build up (**BU**) inside the shielding. The dose build up factor ($B_i >> 1$) depends on photon energy, physical properties of the shielding material, thickness and exposure geometry. The shielding thickness and photon mass attenuation coefficient of the shielding material corresponding to "i" energy bin (Figure 7) are represented by "t" and "$\mu_i$" respectively [**13**].

## Shielding Materials under Investigation

The physical properties of shielding materials to be used in XFEL project are shown in **Table 1**.

**Table 1:** Physical properties of the shielding materials [**14, 15**] under this investigation.

| Shielding Material | Component Nuclide | Weight Fraction | Density: [g.cm$^{-3}$] |
|---|---|---|---|
| Industrial Lead | Pb | 0.96 | 11.3 |
| | Sb | 0.04 | |
| Carbon Steel | C | 0.005 | 7.8 |
| | Fe | 0.995 | |
| Heavy Concrete | O | 0.34 | 3.7 |
| | Mg | 0.02 | |
| | Al | 0.01 | |
| | Si | 0.07 | |
| | Ca | 0.05 | |
| | Fe | 0.51 | |

## Irradiation Experiments in FLASH Tunnel

The shielding measurements were carried out in FLASH tunnel at the designated location as shown in Figure 2. Plates of **(a)** Industrial lead- area: 10×10 $cm^2$, thicknesses: 0.1 cm, 0.5 cm, 1.0 cm, 1.5 cm, 2.0 cm and 5.0 cm, **(b)** Carbon steel- area: 15×10 $cm^2$, thicknesses: 0.1 cm, 1.0 cm, 2.0 cm, 4.0 cm, 6.0 cm and 8.0 cm and **(c)** Custom made Heavy Concrete plates [**16**]- area: 30 ×30 $cm^2$, thicknesses: 5.0 cm, 7.0 cm, 10.0 cm, 20.0 cm, 30.0 cm, 40.0 cm and 50.0 cm were investigated. Radiochromic films were used to assess the transmitted photon dose. The photon transmission probability (Shielding Efficacy) of the above materials was calculated as the ratio of entry and egress gamma doses ($D_t/D_0$) and shown in **Figures 9a, 9b** and **9c**. The idealized narrow beam photon attenuation (without build up) which was calculated using Equation (1) and gamma mass attenuation coefficients [**17**], are plotted.

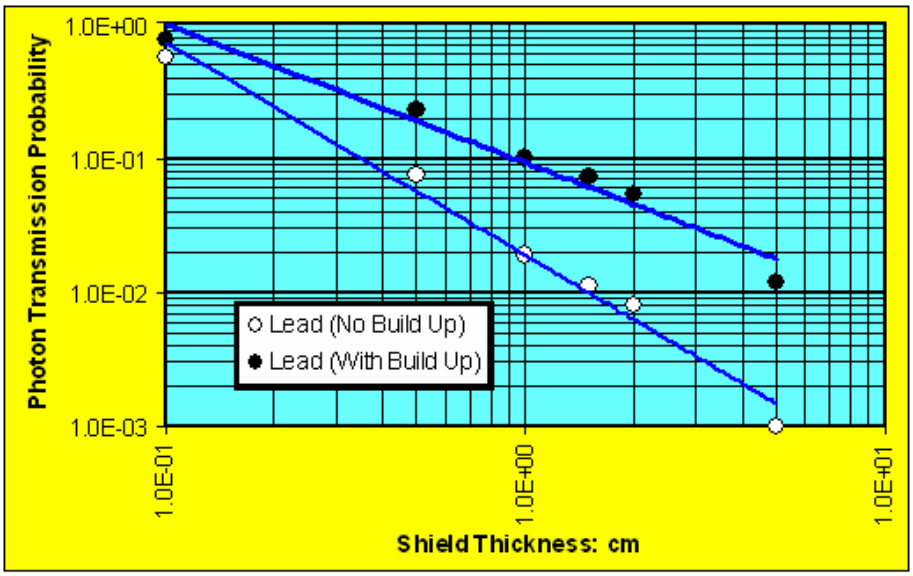


**Figure 9a:** Experimentally estimated photon transmission probability (Shielding Efficacy) of Industrial Lead shown as a function of shield thickness. The transmission probability of narrow photon beam (without build up) calculated using Equation (1) is shown.

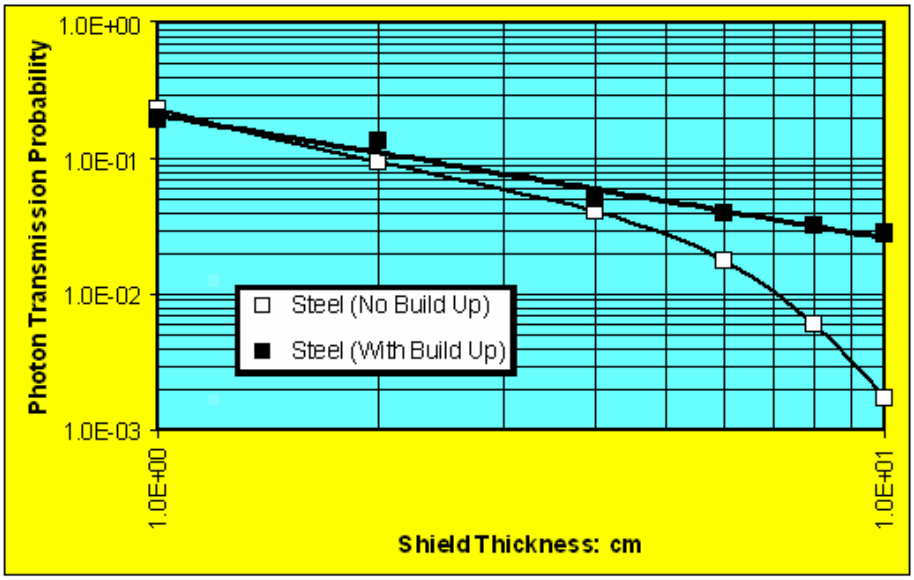


**Figure 9b:** Experimentally estimated photon transmission probability (Shielding Efficacy) of Carbon Steel shown as a function of shield thickness. The transmission probability of narrow photon beam (without build up) calculated using Equation (1) is also shown.

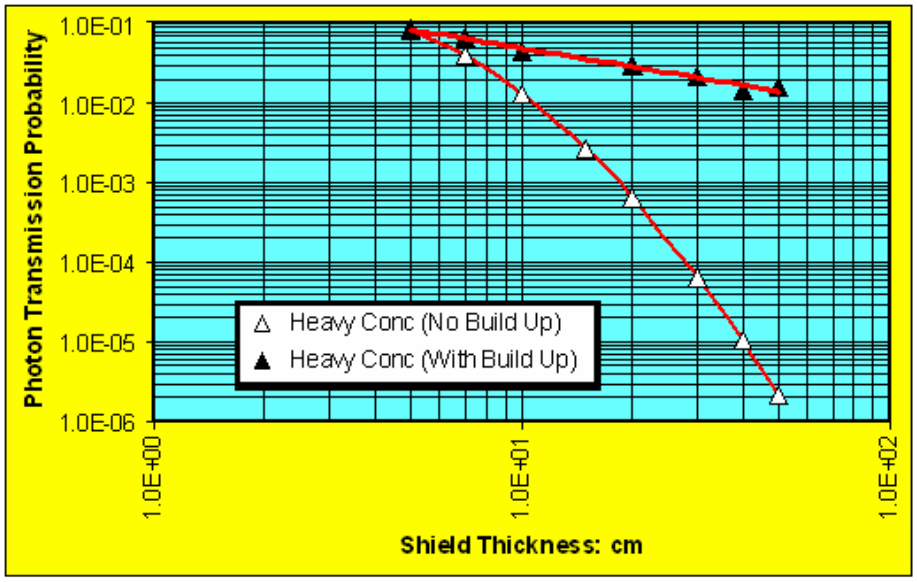


**Figure 9c:** Experimentally estimated photon transmission probability (Shielding Efficacy) of Heavy Concrete shown as a function of shield thickness. The transmission probability of narrow photon beam (without build up) calculated using Equation (1) is shown.

**Fitting of Experimental Data Points**

For the purpose of practical and user-friendly applications by shielding engineers the data points of the photon transmission probability curves (with build up), presented in **Figures 9a, 9b** and **9c** were fitted with specific power functions (**Figure 10**).

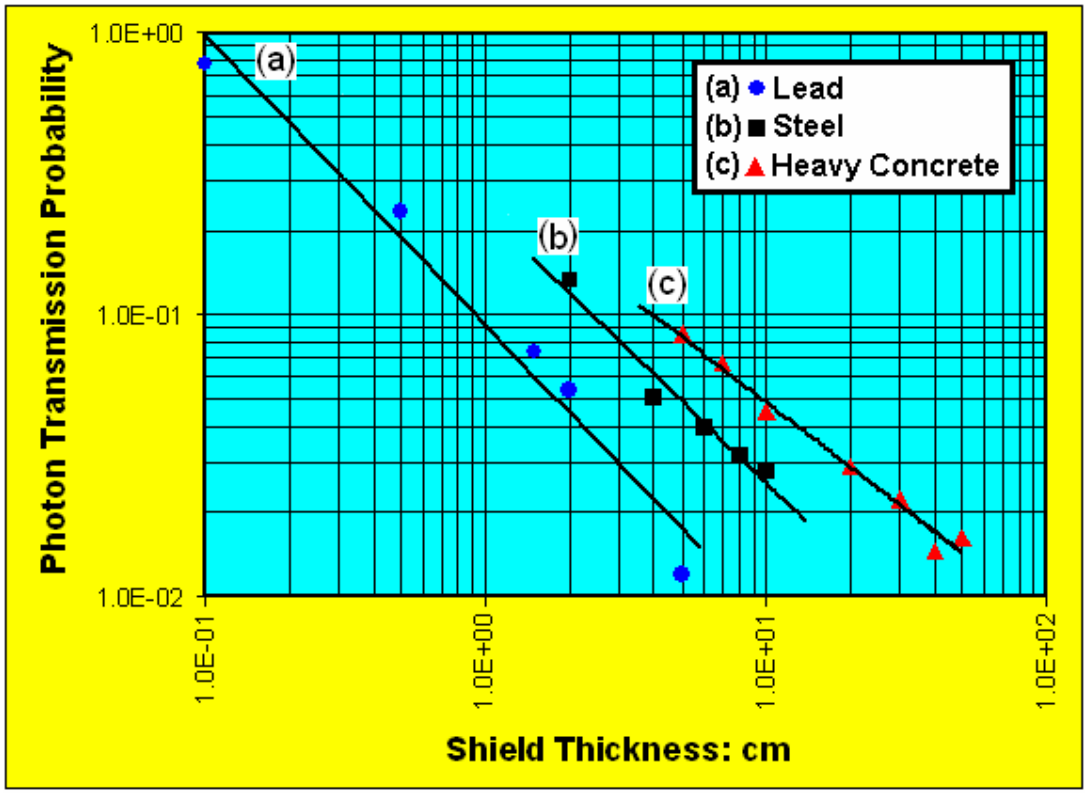


**Figure 10:** Showing the power function fittings of the experimentally estimated broad beam photon transmission probability curves for **(a)** Industrial Lead: $y = 0.0916x^{-1.03}$, [$R^2 = 0.97$] **(b)** Carbon Steel: $y = 0.232x^{-0.961}$, [$R^2 = 0.96$] and **(c)** Heavy Concrete: $y = 0.286x^{-0.766}$, [$R^2 = 0.98$].

**Multi-Layer Shielding**

High density shielding materials followed by a low density material allow reducing the overall build up factor. This effect has been reported in the reference [**18**] and rigorously dealing with "Lead/Water" and "Iron/Water" layer combinations, exclusively relevant to nuclear reactor shielding. Furthermore, an accurate evaluation of build up factors of multi-layer shielding requires many exposure-geometry specific numerical parameters depending on photon energy distribution and shield dimension. As those data sets were not available to us, we have carried out dedicated experiment with "Lead/Heavy Concrete" combination using the realistic (experimentally evaluated) photon energy distribution (**Figure 7**) at FLASH. Photon transmission probabilities for 0.5 cm, 1.0 cm and 2.5 cm thick lead shield followed by 10 cm and 20 cm thick heavy concrete were evaluated. Radiation dosimetry was carried out using Gaf-EBT type radiochromic films as described above. Results are shown in **Figure 11**.

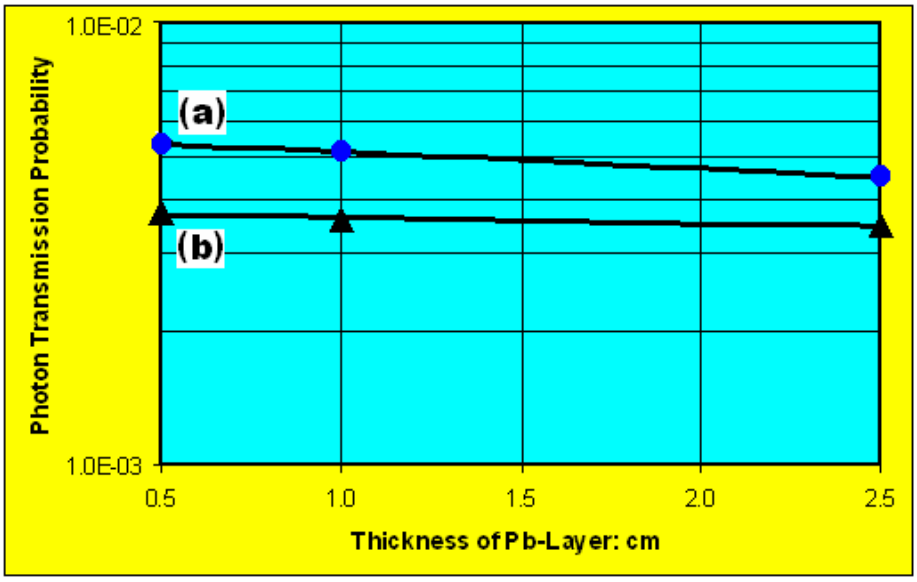


**Figure 11:** Photon transmission probability in "Industrial Lead/Heavy Concrete" multi-layered shield evaluated using the realistic photon radiation field at FLASH. The power function fitting curves are also given: **(a)** Lead followed by 10 cm Heavy Concrete: y = -0.000425x + 0.00555, [$R^2$ = 0.98], **(b)** Lead followed by 20 cm Heavy Concrete: = -0.000109x + 0.00374, [$R^2$ = 0.94].

## SUMMARY AND CONCLUSIONS

Primary objective of this project is to estimate the photon attenuation properties in industrial lead, carbon steel and heavy concrete. Those materials will be used to construct radiation shielding for the racks to accommodate the sensitive electronic devices. The racks should be installed in the narrow space of a cross section of 1.1×1.7 $m^2$ available in the 5 m diameter XFEL tunnel (Figure 1). It is therefore, imperative to implement a highly optimised shielding which provides maximum photon attenuation with a minimum thickness.

The XFEL tunnel will be jam-packed with a multitude of objects, such as accelerator modules, utility ducts, conduits, electrical power and signal cables, crates, RF wave guides etc., which makes a reliable and accurate Monte-Carlo simulation of the photon transmission in the shielding (i.e. determination of shielding efficacy) impossible. Hence, we have carried out experimental estimation of the shielding parameters (photon attenuation characteristics) at FLASH, taking into account the realistic situation, i.e. energy and spatial distributions of photons.

These assumptions are justified, because the XFEL linac will be based on the same superconducting TESLA cavities as FLASH. Furthermore, the radiation environment of XFEL is expected to be quite similar to that of FLASH.

The photon transmission probabilities (shielding efficacy) of industrial lead, carbon steel, heavy concrete as well as multi-layer shield made of industrial lead and heavy concrete were estimated. A two-layer shield made of 0.5 cm industrial lead followed by 10 cm heavy concrete found to be optimum (**Figure 12** and **Table 2**).

The experimental data points are optimally fitted with power and linear functions. The relevant fitting parameters are presented for extrapolation of the photon transmission probability (shielding efficacy) for any selected shield thickness (**Table 3**).

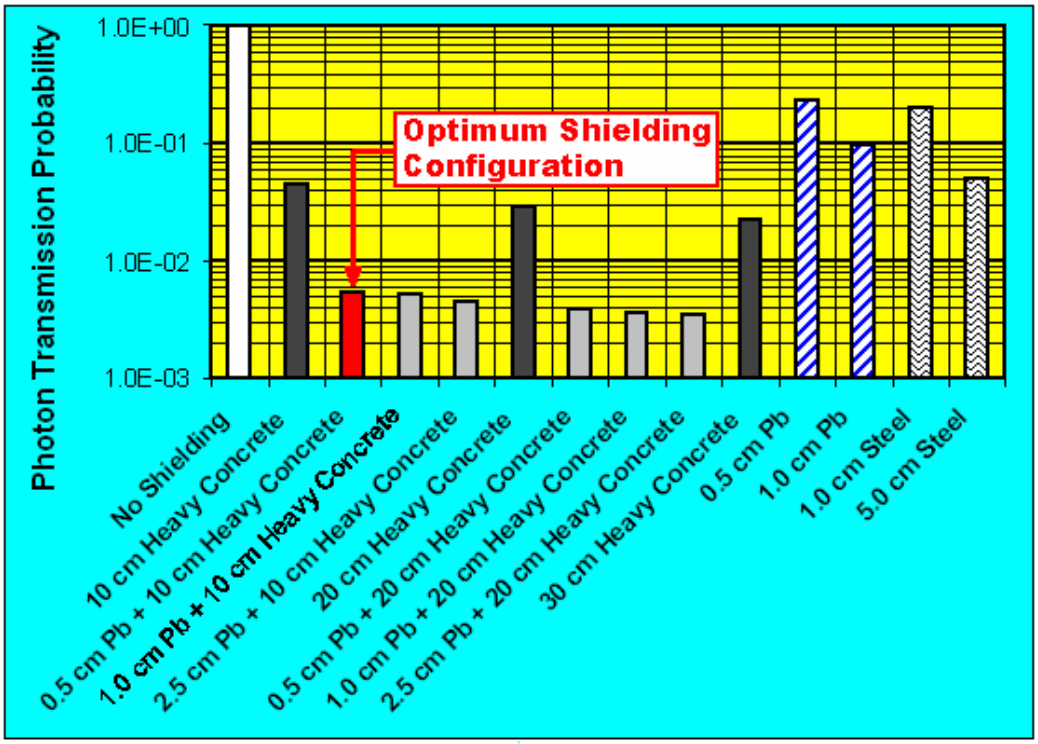


**Figure 12:** Experimentally estimated photon transmission probability (PTP) of industrial lead, carbon steel and heavy concrete. The PTP of multi-layer shielding made of industrial lead and heavy concrete of various thicknesses are also depicted. The optimum shielding configuration is indicated.

**Table 2:** Showing the experimentally estimated photon transmission probability (PTP) of the shielding materials for XFEL. The optimum shielding configuration (0.5 cm industrial lead followed by 10 cm heavy concrete) is highlighted.

| Shielding Material | Density: g.cm$^{-3}$ | Thickness: cm | PTP |
|---|---|---|---|
| Industrial Lead (IL) | 11.3 | 0.5 | 0.234 |
| | | 1.0 | 0.092 |
| Carbon Steel | 7.8 | 1.0 | 0.20 |
| | | 5.0 | 0.05 |
| Heavy Concrete (HC) | 3.7 | 10 | 0.045 |
| | | 20 | 0.029 |
| | | 30 | 0.022 |
| (IL) Followed by [HC] | --- | (0.5) + [10] | 0.0053 |
| | --- | (1.0) + [10] | 0.0051 |
| | --- | (2.5) + [10] | 0.0045 |
| (IL) Followed by [HC] | --- | (0.5) + [20] | 0.0037 |
| | --- | (1.0) + [20] | 0.0036 |
| | --- | (2.5) + [20] | 0.0035 |

**Table 3:** Showing the fitting functions and the fitting parameters for the estimation of shielding efficacy Y for any given shield thickness X [cm].

| Shielding Modality | a | b | $R^2$ | Function |
|---|---|---|---|---|
| Industrial Lead (IL) | 0.916 | -1.03 | 0.97 | $Y = aX^b$ |
| Carbon Steel | 0.232 | -0.961 | 0.96 | |
| Heavy Concrete (HC) | 0.286 | -0.766 | 0.98 | |
| IL* followed by 10 cm HC | -0.000425 | 0.00555 | 0.98 | $Y = aX + b$ |
| IL* followed by 20 cm HC | -0.000109 | 0.00374 | 0.94 | |

IL* represents the variable, i.e. the thickness of the industrial lead layer X [cm].

## ACKNOWLEDGEMENT

Authors wish to thank Dr. Christopher Gerth, DESY MPY group for reviewing this report and many valuable comments and suggestions relevant to practical application of these results in the design and construction of radiation shielding of XFEL.

## REFERENCES

**[1]** XFEL Technical Design Report, July 2007.

**[2]** H J Eckoldt, DESY MKK6 Group, Private communication, May 2008.

**[3]** K Rehlich, DESY MSK Group, Private communication, June 2008.

**[4]** B Mukherjee, D Rybka, D Makowski, T Lipka and S Simrock. Radiation measurement in the environment of FLASH using passive dosimeters. Meas. Sci. Technol. 18 (2007) 2387.

**[5]** B Mukherjee and S Simrock. Radiation dosimetry at free electron lasers in Hamburg. Radiat. Meas. 43 (2008)1154.

**[6]** B Mukherjee, D Makowski, P Krasinski, P Cross, M Grecki and S Simrock. Novel applications of radiochromic film in radiation dosimetry at high energy accelerators. Proc. 15th International Conference on Mixed Design (MIXDES 2008), 19-21 June 2006, Poznan, Poland.

**[7]** B Mukherjee, M Valentan, D Makowski, D Rybka and S Simrock. Radiation field unfolding at the Free Electron Laser in Hamburg (FLASH) using a Genetic Algorithm. Proc. International Conference on Computer as a Tool (EUROCON 2007), 9-12 September 2006, Warsaw, Poland.

**[8]** H Dinter, B Racky and K Tesch. Neutron Gamma dosimetry at high energy accelerators. DESY Internal Report: DESY D3-82, January 1996.

**[9]** A M Ougouuag J G Williams M B Danjaji S Yang and J L Mason. Differential displacement kerma cross sections for neutron interaction in Si and GaAs. IEEE Trans. Nucl. Sci. 37(1990)2219.

**[10]** B Mukherjee and S Simrock. Characterisation of the bremsstrahlung generated by a 450 MeV superconducting electron linac using the inverse calculation method based on a genetic algorithm. Radiat. Meas. 42(2007)1355.

**[11]** B Mukherjee, S Simrock and S Tripathy. Deconvolution of bremsstrahlung spectrum at the superconducting TESLA accelerator module using inverse calculation method. Proc. International Conference on Computer as a Tool (EUROCON 2007), 9-12 September 2006, Warsaw, Poland.

**[12]** B Mukherjee E Negodin, T Hott and S Simrock. Prediction of radiation levels at critical locations of the future European XFEL using the radiation measurement data from FLASH. IEEE NSS Conference 19-23 October 2008, Dresden Germany (accepted).

**[13]** T M Jenkins, Shielding of Photons for SPEAR, SLAC-TN-71-5, March 1971**.**

**[14]** H Dinter and K Tesch. Calculation of the Shielding for the Storage Ring DORIS. DESY Internal Report: DESY D3-10, June 1972.

**[15]** P F Sauermann. Radiation Protection by Shielding. Verlag Karl Thiemig, Munich 1976.

**[16]** B Mukherjee, D Makowski, D Rybka, O Kroeplin, S Simrock and H J Eckoldt. External radiation shielding for the protection of electronic devices operating in the FLASH facility tunnel at DESY. Proc. 13th International Conference on Mixed Design (MIXDES 2006), 22-24 June 2006, Gdynia, Poland.

**[17]** X-Ray Mass Attenuation Coefficients. National Institute of Standards, Washington D C, USA http://physics.nist.gov/PhysRefData/XrayMassCoef/cover.html

**[18]** A Assad, M Chiron, J C Nimal, C M Diop and R Ridoux. A new Approximating Formula for Calculating Gamma-Ray Buildup Factors in Multiplayer Shields. Nucl. Sci. Eng. 132(1999)203.